1.1. Perovskites

The materials having crystal structure resembling calcium titanate ($CaTiO_3$) are called as perovskite oxides. The perovskite derived from mineral which was discovered in Urai mountain of Russia in 1839 by Gustav Rose. The name perovskite was taken from the Russian Mineralogist L. A. Perovski (1792-1856). General chemical formula of perovskite oxide is ABO_3 where A and B are cations having different sizes (A greater than B) and O is anion [Giaquinta and Loye (1994), Pena and Fierro (2001)]. The structural representation was shown in Figure 1.1. The metal ions present at B site is mainly 3d, 4d, 5d transition metals which was octahedral (BO_6) surrounded by oxide ions whereas A site occupied by alkaline earth metals [Vasala and Karpinen (2015)].

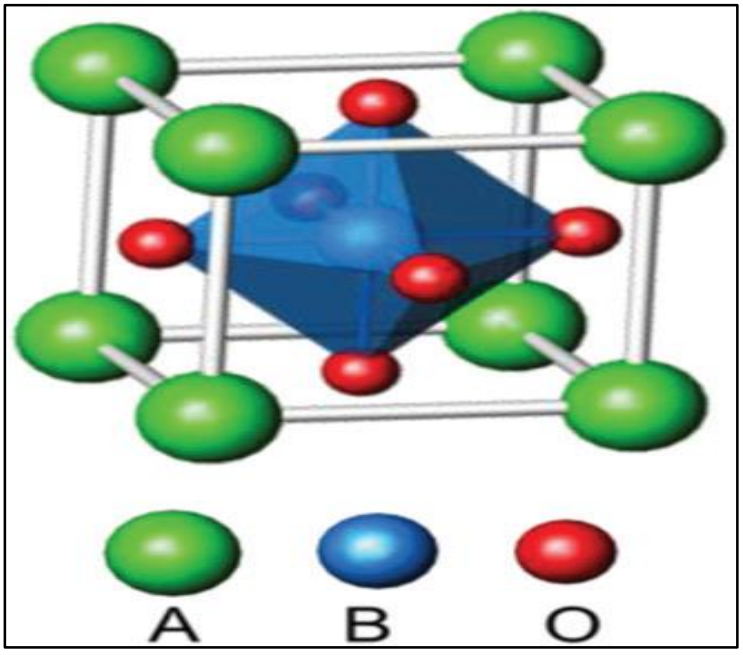

Figure 1.1 The ABO_3 Perovskite structure [Rabuffetti and Brutchey (2014)]

`

According to Goldschmidt the geometrical requirement for the formation of perovskite structure is that the ionic radii r_A, r_B and r_O of cations A, B and anion O, respectively, must satisfy the following given relation as shown in equation (1.1):

$$t = \frac{(r_A + r_O)}{\sqrt{2}(r_B + r_O)} \qquad (1.1)$$

where t is the tolerance factor, which describes the range of relative sizes for which the perovskite structure is stable. The structure will be cubic if $0.95 < t \leq 1.0$. Compounds having tolerance factor in the range $0.75 \leq t \leq 0.95$ are non-ferroelectric with distorted structure while those with ≥ 1.0 are ferroelectric and hexagonal [Wood (1951), Singh *et al*. (2014)]. If $t < 0.75$, the compound does not crystallize in perovskite structure. They also have some empirical rules for the stability of ABO_3. $ACu_3Ti_4O_{12}$ is a group of perovskite oxide in which at A Site Ca, Ba and Sr whereas at B site shared by both Copper and Titanium metal ions [Deschanvres *et al.* (1967)]. $ACu_3Ti_4O_{12}$ type perovskites shows complex perovskite structure which has very interesting dielectric constant that was responsible for its applications. Relaxor ferroelectric materials like $Pb(Mg_{1/3}Nb_{2/3})O_3$ [PMN] [Swartz *et al*. (1984)], $Pb(Zn_{1/3}Nb_{2/3})O_3$ [PZN] [Halliyal and Safari. (1994)], and $Pb_{1-x}La_x(Zr_{1-y}Ti_y)O_3$ [PLZT] has high dielectric constant (ε_r) ~ 1000-20,000 but these materials were not environment friendly due to lead content. $ACu_3Ti_4O_{12}$ type oxides which have complex perovskite structure are well known for their ability to produce high dielectric constant [Ramirez *et al*. (2000), Subramanian *et al*. (2000)] this has led to many important applications. Presently, we use $BaTiO_3$ or relaxor ferroelectrics such as $Pb(Mg_{1/3}Nb_{2/3})O_3$ (PMN) [Yoshida *et al.* (1998)], $Pb(Zn_{1/3}Nb_{2/3})O_3$ [PZN], and $Pb_{1-x}La_x(Zr_{1-y}Ti_y)O_3$ [PLZT] [Moulson and Herbert (2003)] which are not environment friendly as capacitor materials (dielectric constant (ε_r) ~ 1000-20,000). Barium titanate is a well-known

ferroelectric and multilayered dielectric material [Hennings (1987)]. $BaTiO_3$ was first discovered during Second World War (1941-1944) in U. S. A, Russia and Japan. Firstly, BaO doped TiO_2 synthesized for enhancement of dielectric constant of material. The Erie and Resistor Company found dielectric constant more than 1000 which was nearly ten times greater than TiO_2. The dielectric anomaly of Bao-TiO_2 demonstrated by ferroelectric switching in ceramics [Von *et al.* (1946)]. The detailed structural study of barium titanate was carried out by Miyake and Ueda in 1946. The curie temperature of barium titanate was 120 ^{0}C indicating tetragonal to cubic phase transition which causes significant dielectric constant [Petrovsky *et al.* (2008)]. The grain size of polycrystalline $BaTiO_3$ affected its dielectric properties. Enhanced dielectric constant of barium titanate observed at grain size coming under 1μm [Frey and Payne (1996), Kanata *et al*. **(**1987)]. Such increment in dielectric constant was due to twin behavior of polycrystals and decrease in grain size. Despite ability of twin mechanism reduce the bulk strain energy present in homogeneous transformations; such type of stress is still present near the grain boundary for larger grain ceramics. To reduce residual strain energy ultimately contributes resulting twin structure [Jacobs (1995)].

1.2. High dielectric constant ABO_3 perovskites

1.2.1. Barium Titanate ($BaTiO_3$)

The high dielectric constant of barium titanate is responsible for its ferroelectric behavior [Arlt and Sasko (1980)]. Almost same ionic radii of Barium and oxygen 1.4 Å and make a face centered cubic arrangement of atoms. Ti^{4+} ions are present at B-site of perovskites which is octahedrally surrounded by six oxygen ions. TiO_6 octahedra in barium titanate shift either up or down, this is the responsible factors for ferroelectricity [Aimi *et al*. (2014)]. High oxidation state and low laying d- orbital of titanium creates electronic polarization and atomic

arrangement around it. On cooling, three ferroelectric phase transitions are observed involving atomic movement of 0.10 Å in $BaTiO_3$. These transition effects the direction of spontaneous polarization from one phase to other. For greater than 1450 ^{0}C non ferroelectric hexagonal [Kay and Vousden (1949)], whereas bellow 1450 ^{0}C cubic form exists, which are paraelectric in nature. Tetragonal form of barium titanate exists at room temperature with axial ratio c/a ≈ 1.012 [Jaffe *et al.* (1971), Yashima *et al*. (2005)]. $BaTiO_3$ shows strong temperature dependent dielectric constant at Curie temperature.

1.2.2. Calcium-Titanate ($CaTiO_3$)

The behavior of calcium titanate is paraelectric at room temperature having poor dielectric properties. Donor doping increase the internal boundary layer effect which improves its dielectric constant. Concentration of dopant and sintering atmosphere also monitors dielectric permittivity of materials. Doping of Yttrium (≤0.75 mol %) and sintering of these sample in nitrogen atmosphere gives very high dieletric constant with relaxor behavior [Neirman and Burn (1984)]. The symmetry of calcium titanate is temperature dependent at room temperature orthorhombic and become tetragonal at 600 ^{0}C, which convert into cubic symmetry at 1000 ^{0}C. Electrical conductivities in oxidizing atmosphere at 130 ^{0}C show p-type semiconductor behavior [Cox and Tredgold (1967)].

1.2.3. Strontium Titanate ($SrTiO_3$)

$SrTiO_3$ is mainly used as high temperature superconductor thin films [Chen *et al.* (1988)], in photolysis of water, oxygen sensor and in magneto-hydrodynamic operators [Butler *et al.* (1981), Chang *et al.* (1983)], memory devices, optical processors [Kiss and Phillips (1969), Bernay and Cowan (1981)]. Oxygen vacancy of this material is responsible for n-type

conductivity [Walters and Grace (1967)]. The symmetry of $SrTiO_3$ is cubic at room temperature with band gap 3.2 eV [Mattheiss (1972), Pertosa *et al.* (1978)] and paraelectric [Mitsui and Westphal (1961)]. Trivalent rare earth metal ions doped strontium titanate shows high dielectric constant and relaxor behavior. Dielectric constant of pure strontium titanate is around 300 whereas Yttrium doping improves it to 18000.

A list of perovskite oxides along with their dielectric constant and application of perovskites are shown in Table 1.1 and Table 1.2 respectively.

Table 1.1 Dielectric constants of various ceramic materials are tabulated

S. No	Composition	Dielectric constant	References
1	$CaCu_{2.70}Mg_{0.30}Ti_4O_{12}$	$3.42x10^5$	[Singh *et al.* (2013)]
2	$NiFe_2O_4$/MWCNT	1.06×10^5	[Soomro *et al.* (2017)]
3	$Na_{0.5}K_{0.5}NbO_{3+x}CuF_2$	250,000	[Weng *et al.* (2017)]
4	$0.5Bi_{2/3}Cu_3Ti_4O_{12}$-$0.5Bi_3LaTi_3O_{12}$	$13.94x10^3$	[Gautam *et al.* (2017)]
5	$Ba_6Y_2Ti_4O_{17}$(BYTO)	$1.5\ x10^3$	[Yadava *et al.* (2016)]
6	Eu_2CuO_4	$5x10^3$	[Salame *et al.* (2014)]
7	T-type La_2CuO_4	10^3	[Salame *et al*. (2016)]
8	$0.5BaTiO_3$–$.5Bi_{2/3}Cu_3Ti_4O_{12}$	43459	[Khare *et al*. (2017)]
9	Ca[($Li_{1/3}Nb_{2/3}$)1exTix]O3	40,000	[George and Sebastian (2008)]
10	$Ba(Fe_{0.5}Nb_{0.5})O_3$-$Bi_{0.2}Y_{2.8}Fe_5O_{12}$	30000	[Yang *et al*. (2017)]
11	$Ba_{0.75}Sr_{0.25}TiO_3$	~24,000	[Huang *et al.* (2008)]
12	$CaCu_3Ti_4O_{12}$	20,000	[Tuichai *et al.* (2013)]
13	$K_{0.5}Na_{0.5}NbO_3$	20,000	[Bobnar *et al.* (2009)]
14	$Ba_4Sm_{9.33}Ti_{18}O_{54}$	~10,000	[George *et al.* (2009)]
15	$Bi_{1.5}ZnNb_{1.5}O_7$	10,000	[George *et al.* (2007)]
16	lead-lanthanum-zirconate-titanate	7819	[Limpichaipanit and Ngamjarurojana (2017)]
17	$Y_{2/3}Cu_3Ti_{3.95}In_{0.05}O_{12}$	5068	[Singh *et al.* (2016)]
18	$(Ba_{0.95}Ca_{0.05})$ $(Ti_{0.96}Zr_{0.04})O_3$	3910	[Yang *et al.* (2011)]
19	$(Bi_{0.5}Na_{0.5})_{1-x}Yb_xTiO_3$	1357	[Han *et al*. (2017)]

Table. 1.2 Applications of Perovskite oxides and complex perovskite oxides

S. No	Ceramics	APPLICATION	References
1	$BaTiO_3$	Multilayer Capacitor	[Park (2005)]
2	$Pb\ (Zr_x\ Ti_{1-x})O_3$	Piezoelectric Transducer	[Lendermann *et al.* (2004)]
3	$BaTiO_3$	P. T. C. Thermistor	[Affleck and Leach (2005)]
4	(Pb, La) (Zr, Ti)O_3	Electrooptical Modulator	[Nakada *et al.* (2003)]
5	$BaZrO_3$	Dielectric Resonator	[Wakino *et al*. (1986)]
6	$Pb\ (Mg_{1/3}\ Nb_{2/3})O_3$	Elecrostrictive Actuator	[Takagi *et al.* (1993)]
7	Ba(Pb, Bi) O_3 layered cuprates	Superconductor	[Grumann *et al.* (1994)]
8	$GdFeO_3$	Magnetic Bubble Memory	[Söderlind *et al*. (2009)]
9	$YAlO_3$	Laser Host	[Stefaniuk *et al.* (2006)]
10	(Ca, La)MnO_3	Ferromagnet	[Heffner *et al.* (2000)]
11	$SrCeO_3$	Hydrogen sensor	[Iwaraha *et al.* (1981)]
12	$BaCeO_3$	Hydrogen sensor	[Iwaraha *et al.* (1988)]
13	$BaZrO_3$	H_2 production/ extraction	[Yamanaka *et al.* (2003)]

1.3. Dielectric and Dielectric constant

The dielectric materials also called as dielectric (coined by William Whewell) is electrically insulator which can be polarized by applied electric field. On application of electric field, a little shift in equilibrium position of electric charge, resulting dielectric polarization. The positive and negative charge oriented oppositely in the dielectrics, which creates internal electric field. The dielectric has very high polarizability whereas insulators have low electrical conduction [Ortiz *et al*. (2009)]. Capacitor is the main example of dielectric materials in which these materials placed in two metallic plates. As the strength of external applied electric field increases polarization of dielectric also increase. Permittivity is a material property that affects the coulomb force between two point charges in the material [Harvey (1989)]. The strength of electric field between charges decreased relative to vacuum by a factor known as relative permittivity (equation (1.2)). The term dielectric constant commonly used in place of relative permittivity in physics, engineering and chemistry.

$$\varepsilon_r = \frac{\varepsilon}{\varepsilon_0} \qquad (1.2)$$

Where $\varepsilon_r(\omega)$ is the relative permittivity of the material, $\varepsilon(\omega)$ is the complex frequency dependent absolute permittivity and ε_0 is the permittivity of free space (vacuum permittivity). Relative permittivity is a dimensionless property have complex valued. The real (ε_r') and imaginary (ε_r'') parts of dielectric constant are formulated in equation (1.3) [Paik *et al.* (2014)].

$$\varepsilon_r = (\varepsilon_r') - i\varepsilon_r'' \qquad (1.3)$$

At zero frequency, relative permittivity of material is known as static relative permittivity [Suresh (2013)]. Dielectric constant can be calculated from capacitance and conductance relation given in equation (1.4).

$$\varepsilon_r = \frac{C \times l}{\varepsilon_0 \times A} \tag{1.4}$$

Where, C represents capacitance of material, l and A are thickness and area respectively of the cylindrical pellets. When a material is kept in an electric field, it will respond in differently depending on the type of material. Conducting materials have loosely bonded valence electrons that can be excited by thermal energy. When a conductor is acted upon by an electric field, the loosely bonded electrons are free to move between the molecules within the material. In choosing a capacitor material, the electron bonds within the material needs to be strong enough, not allow electrons to move between molecules. In an insulating or dielectric, the material has electron bonds that are stronger than that of conducting materials. When an insulating material or a dielectric material is exposed to an electric field, the valence electrons are not allowed to move between molecules of the material. There is a point at which the energy is large enough to break the electronic bonds, which is called intrinsic breakdown and will be discussed in a later section [Todd and Shi (2003)].

1.4. Polarization

When an electric field is applied to an insulator, the electronic distribution and the nuclear positions are altered and the charges in the molecules are displaced. This displacement creates small electric dipoles within the material. Electric dipoles are atomic structures that have a difference in charge from one end to the other. As opposed to a conductor, the displaced charges, also called bound charges, do not escape the molecules. This displacement can be

thought of as two opposite charges, which are separated by a distance. The dipole can be represented by a vector that points from the negative charge to the positive charge and has a magnitude of the distance between them. This vector is called as electric dipole moment. The direction of the dipole moment is always in the direction of the applied field. The amount of polarization (P) depends on the electric field (E) and the quantity called the polarizability α, which is shown in equation (1.5).

$$P = \alpha \mathrm{E} \quad (\mathrm{C/m^2}) \tag{1.5}$$

The electric displacement (D) is the total charge displacement induced in the material. The mathematical expression of electric displacement given by Maxwell is as shown in following equation (1.6).

$$D = \varepsilon_0 E + P \quad (C/m^2) \tag{1.6}$$

Electric displacement generates by the combined effect of applied electric field and induced electric field by polarization.

1.5. Substitution in perovskites

The dielectric properties of perovskites are tailored by substitution of some other metal ions which improve its technological application of material [Fouskova and Cross (1970), Bhalla *et al.* (2000), Bhusan *et al.* (2009)]. The dielectric constant is sensitive towards dopants because of shifting in the position of metal ions from their close packed structures and change in the bond length of metal-oxygen bond, which enhances the dielectric properties. The incorporation of dopant metal ions at A and B site of perovskite ABO_3 is useful for tuning of dielectric properties. The difference in size between the dopant and metal ions already present

in perovskite at A or B site is less than 15% then the condition is favorable. If size difference increase, then structural deformation and phase changes may occur due to hindrance. On the basis of valence state of metal ions substitution are of the following types:

1.5.1. Isovalent substitution

If the valency of dopant and ion which it partially or completely replaced by it are same, such type of doping known is known as isovalent substitution. For example, in $CaTiO_3$ partial/complete substitution of Ca^{2+} by Ba^{2+}, Sr^{2+}, Pb^{2+}, whereas Ti^{4+} substituted by Zr^{4+}, Sn^{4+}, and Hf^{4+}.

1.5.2. Heterovalent substitution

If the valency of dopant and ions which are partially or completely replaced by it are different, such type of doping known as heterovalent substitution. Such type of substitution creates defects in perovskite material due to unbalance charges. Heterovalent substitution is possible at both A and B site of ABO_3 perovskite. This substitution is of two types:

(a) Acceptor Substitution

The oxidation state of dopant is lower than that of A or B site ions called as acceptor dopant. Such type of substitution creates holes which replace or generate oxygen vacancies. Examples, Na^{+} substitute Ba^{2+}, Cu^{2+} substitutes Ti^{4+}.

(b) Donor Substitution

In this substitution, oxidation state of dopant is higher than that of A or B site ions called as donor dopant. The higher valency of dopant increases effective positive charge on material which was neutralized by effective negative charge, electrons or cation vacancy examples, La^{3+} or Y^{3+} on Ba^{2+} [Zhi *et al*. (1999)] and Nb^{5+} on Ti^{4+} site in barium titanate separately.

1.6. Chemical synthesis methods of ceramic materials

Most of the ceramic materials are synthesized by conventional solid state method in which stoichiometric ratio of all metal cations are taken in agate and mortar grind the mixture with the help of suitable solvents like acetone or ethanol. Calcination of material was done with the intermediate grinding and pressing to make it in a fine powder. The ceramic pellets are prepared with the help of binder polyvinyl alcohol. These pellets are heated slowly to remove binder, afterwards annealing was performed at higher temperature at controlled heating rate followed by cooling. This synthesis method has taken relatively long reaction time and high temperatures. The complete homogeneity of reaction mixture is not obtained even several times of grinding results in the formation of some secondary phases. In micro levels, homogeneity is not observed in solid state method. On the other hand, atomic level mixing of reaction components provided by wet chemical method resulting formation of nanocrystalline materials at relatively low temperature and time duration compared to solid state method. There are many chemical methods, such as sol-gel, co-precipitation and hydrothermal processes [Jha *et al* (2003), Liu *et al* (2007), Masingboon *et al* (2008)] which were widely used for the synthesis of ceramic materials. The capacitor industries prepare titanates and niobates using Pechini's method. The modified Pechini methods also known as citrate gel

process or amorphous citrate gel process are used for synthesis of perovskite oxide materials. Aqueous solutions of metal precursors are mixed and with the addition of organic compounds having either acid or hydroxyl functional groups like citric acid, glycine, tartaric acid and glycerol which can form complex with metal ions. The reaction mixture was heated to evaporate water completely; resulting highly viscous resin on continuous heating combustion of organic composition takes place. Glycine assisted sol gel process is also one of the combustion method to synthesize ceramic materials. It helps in combustion of viscous mass by ignition of materials to produce powder [Chick *et al*. (1990)]. Glycine is the simple amino acid having both carboxylic and amino group which helps in the formation of complex with metal cations to inhibit precipitation. Glycine plays an important role in ignition step in which it acts as fuel. Ignition step is highly explosive so intense care was required during this period of time. After ignition very fine crystalline powder obtained due to high reaction temperature for a short time and which is in contrast to pechini method, grinding is not required. This method is use for the synthesis of simple and complex oxides like manganites, chromites and ferrites.

1.7. Impedance spectroscopy

Dielectric spectroscopy is also known as impedance spectroscopy in which dielectric properties of materials were measured as a function of frequency. Impedance spectroscopy is based on interaction of external electric field with electric dipole of materials. Internal barrier layer capacitance (IBLC) mechanism is very useful concept for explaining high dielectric constant of ceramic materials [Leret *et al.* (2007)]. According to IBLC model materials having semiconducting grain surrounded by insulating grain boundaries are responsible for high dielectric constant of $CaCu_3Ti_4O_{12}$ [Calvert *et al.* (2006), Chiodelli *et al*. (2004)]. The

interfacial polarization is responsible factor for giant dielectric constant, barrier layers are located between the grain and grain boundary [Liu *et al.* (2005), Liu *et al.* (2007)]. Sinclair *et al.* 2002, used impedance spectroscopy to explain $CaCu_3Ti_4O_{12}$ ceramics are electrically heterogeneous, due to semiconducting grains and insulating grain boundaries. The resistance and capacitance of grain and grain boundary are representing in circuit in which two parallel RC elements connected in series, one RC element corresponding to grains R_gC_b and the other $R_{gb}C_{gb}$ representing insulating grain boundary region. The complex impedance plane plot and equivalent circuit was shown in Figure 1.2 the two semicircles are representing corresponding grain and grain boundary [Adams *et al.* (2006)].

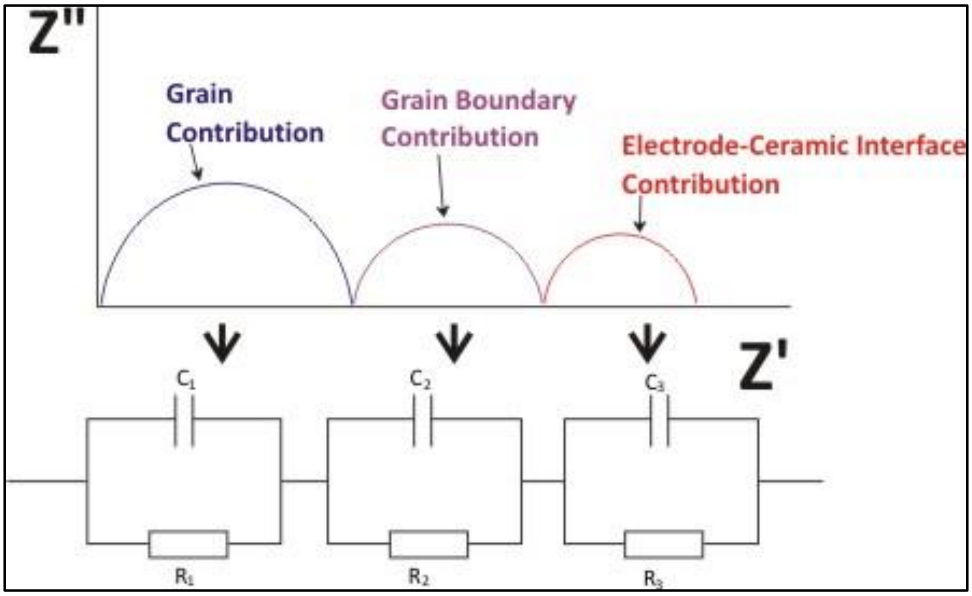

Figure 1.2 Complex impedance plane plot and equivalent circuit

In some cases, semicircle of grains (bulk) or electrode appears at very high frequency is not appearing due to instrument limitation. Impedance spectroscopy reveals the electronic heterogeneity of materials because of semiconducting grain and insulating grain boundaries.

IBLC mechanism supports the high dielectric constant of ceramic materials. The complex impedance can be calculated as from the equation bellow.

$$\boldsymbol{Z^*} = \frac{\mathbf{1}}{\boldsymbol{R_g^{-1}} + i\omega \boldsymbol{C_g}} + \frac{\mathbf{1}}{\boldsymbol{R_{gb}^{-1}} + i\omega \boldsymbol{C_{gb}}} = \boldsymbol{Z' - iZ''} \qquad (1.7)$$

where,

$$\boldsymbol{Z'} = \frac{\boldsymbol{R_g}}{\mathbf{1} + (\boldsymbol{\omega R_g C_g})^2} + \frac{\boldsymbol{R_{gb}}}{\mathbf{1} + (\boldsymbol{\omega R_{gb} C_{gb}})^2} \qquad (1.8)$$

and

$$\boldsymbol{Z''} = \boldsymbol{R_g}\left[\frac{\boldsymbol{\omega R_g C_g}}{\mathbf{1} + (\boldsymbol{\omega R_g C_g})^2}\right] + \boldsymbol{R_{gb}}\left[\frac{\boldsymbol{\omega R_{gb} C_{gb}}}{\mathbf{1} + (\boldsymbol{\omega R_{gb} C_{gb}})^2}\right] \qquad (1.9)$$

Z^*, Z' and Z'' represents complex, real and imaginary impedance, whereas R_g and C_g are the resistance and capacitance of grains. R_{gb} and C_{gb} are the resistance and capacitance of grain boundary. ω represents frequency (ω = 2πf). Dielectric properties of ceramic materials are greatly dependent on grain size [Capsoni *et al.* (2004)] high dielectric constant of (~280000) was found for grain size of 100-300 μm which provides an information regarding extrinsic IBLC mechanism for dielectric response of CCTO ceramic.

1.8. Complex Perovskites

The perovskites oxides having formula $ACu_3Ti_4O_{12}$ (where A = Ca, Sm, Dy, Y and Bi) exhibits many important applications in microelectronics and memory devices. As we know dielectric constant of material is related to polarizability (α), which was created by permanent electric dipole of material which alters its positions on application of external electric field.

The perovskite material having high dielectric constant ($>10^3$) shows ferroelectric characteristic due to presence of permanent electric dipole in absence of applied electric field. Ferroelectric response of materials under high electric field at low temperature does not have macroscopic spontaneous polarization. The materials having temperature dependent dielectric constant is not suitable for many applications. Thermally stable capacitors are used over a wide temperature range. Whereas in case of temperature dependent dielectric constant materials have very limited applications, they fail at variable temperatures. Recently discovered perovskite $ACu_3Ti_4O_{12}$ (A = Ca, Sm, Dy, Y and Bi) shows interesting dielectric constant at room temperature. For calcium copper titanate ($CaCu_3Ti_4O_{12}$) having dielectric constant ($>10^4$) which was frequency independent at the temperature range of 100 - 600 K [Subramanian *et al.* (2000)]. CCTO is very useful material for microelectronic industries. Scientists have been working to improve dielectric properties, particularly to minimize the dielectric loss of high dielectric constant perovskite oxide ($CaCu_3Ti_4O_{12}$) by substituting trivalent or divalent metal ions on A and B sites, respectively. The dielectric response of this material was found to be very sensitive to their microstructure (such as grain size) and processing condition [Bender and Pan (2005)] as well as doping [Chiodelli *et al.* (2004), Capsoni *et al.* (2004)]. People have applied various methods for the synthesis of this material and various cationic substitutions at Cu site, Ti site and both site for the purpose of increasing high dielectric constant and lowering dielectric loss needed for the miniaturization of devices in the modern age of civilization.

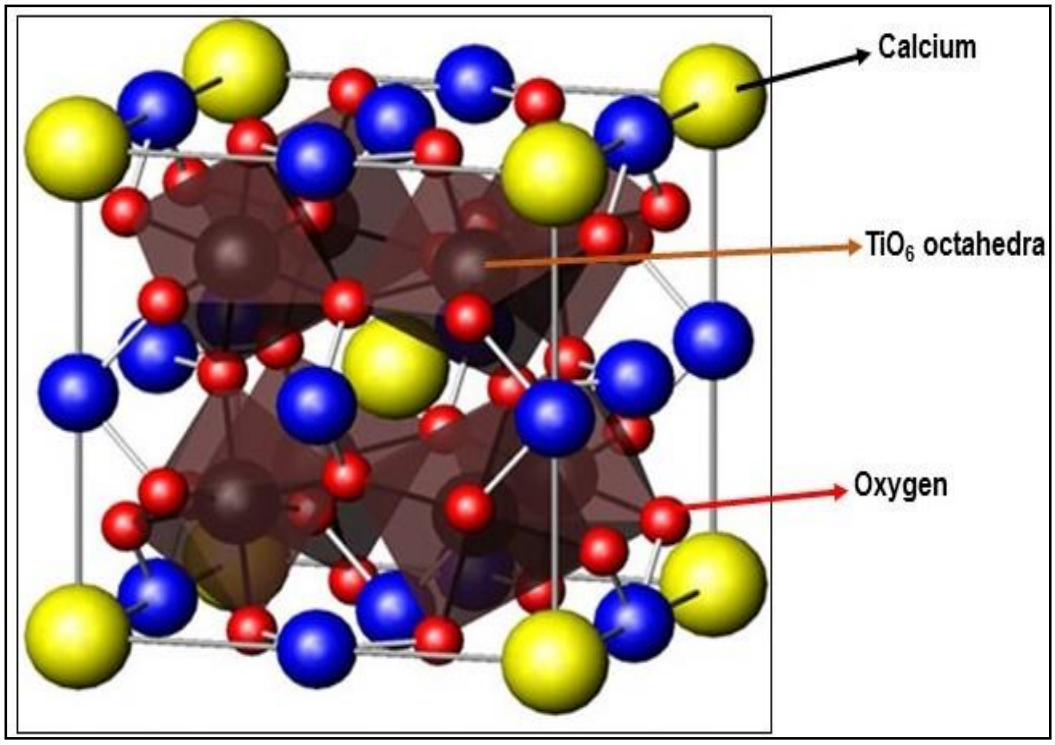

Figure 1.3 Crystal structure of $CaCu_3Ti_4O_{12}$

Structure determination of CCTO has been done by using XRD and neutron powder diffraction studies [Subramanian *et al*. (2000)]. It was found that CCTO crystallizes in a perovskite structure, where Ca^{2+} and Cu^{2+} ions share the A site and Ti^{4+} at the B site. The space group of CCTO is Im3 (cubic system) [Adams *et al.* (2006)] with TiO_6 octahedra present in the structure [Ramirez *et al*. (2000)]. The lattice parameter of this unit cell was found to be 7.391 Å. Structure remains centrosymmetric cubic at very low temperatures. The structure of a unit cell of CCTO is shown in Figure 1.3. Slight deviation in TiO_6 octahedra creates a square planar environment for the Cu^{2+} ions **[**Subramanian *et al.* (2000)]. Each copper atom is bonded to four oxygen atoms and the big Ca atoms are at the corner and body centered positions. Ti^{4+} ions occupy the centrosymmetric position in the octahedral sites. This tilting in TiO_6 octahedra

results enough deviation (141^{o}) to accommodate local distortions, which effectively rules out the pure ferroelectric behavior. In $CaCu_3Ti_4O_{12}$ the observed Ca-O distance is equal to 2.604 Å, which is less than 2.720 Å predicted on the basis of the ionic radii. The strain in Ti-O bond increases the polarizability of the structure. Substitution of donor and accepter on Ca^{2+} and Ti^{4+} sites respectively cause variation in tension due to different ionic radii as compared to the host ions. This will result change in polarizability and hence dielectric constant was observed experimentally. Besides CCTO other complex perovskite also have very high dielectric constant for example, $Bi_{2/3}Cu_3Ti_4O_{12}$ (BCTO), $Y_{2/3}Cu_3Ti_4O_{12}$ (YCTO), $La_{2/3}Cu_3Ti_4O_{12}$ (LCTO) and $Ba_4YMn_3O_{11.5-\delta}$ (BYMO). All these materials show large dielectric constant and exhibits Debye type relaxation and dielectric constant independent on frequency bellow the relaxation frequency. Among these $Ba_4YMn_3O_{11.5-\delta}$ (BYMO) exhibits interesting dielectric properties ($\approx 10^4$) at room temperature [Barbier *et al* (2012)]. Many scientists were working for improvement of dielectric constant and reduction in dielectric loss by synthesis route as well as substitution of metal ions having similar or different oxidation states at barium and manganese positions. Doping of copper at manganese site enhances dielectric constant and reduces dielectric loss of BYMO ceramic [Barbier *et al* (2013)]. Substitution at A and B sites of BYMO ceramic creates structural changes tilting and shifting in position of BO_6 octahedra is responsible for improvement in dielectric constant. The dielectric constant is very sensitive to their microstructure (grain size and grain boundary) and processing conditions as well as amount of doping. Researchers have applied various synthesis methods for the formation of this material and substitution at Ba site, Mn site and both site for increasing dielectric constant and lowering dielectric loss which was needed for miniaturization of device in the modern age of civilization.

1.9. Structure of $Ba_4YMn_3O_{11.5\pm\delta}$

The structure of BYMO has been determined using XRD and neutron powder diffraction studies [Kuang *et al.* (2006)]. It has been found that BYMO comes under the perovskite structure $Ba_4REMn_3O_{12}$ (RE= Ce^{4+}, Pr^{4+}) [Fuentes *et al.* (2004)] $Ba_4YMn_3O_{11.5}$ adopts 12R-type hexagonal perovskite structure having BaO_3 stacking $(cchh)_3$ sequence along the c axis, with Mn_3O_{12} face sharing trimers joined through corner sharing with YO_6 units as shown in Figure 1.4. Rietveld refinement and neutron diffraction data reveals the hexagonal structure having $R\bar{3}m$ space group. The refined ND data gives oxygen content and atomic displacement parameters. The transformation of 12-layers hexagonal perovskite $Ba_4YMn_3O_{11.5}$ having oxidation state of manganese (Mn^{4+}) in to 6-layer hexagonal perovskite $Ba_4YMn_3O_{11.5-\delta}$ with mixed oxidation state $Mn^{3+/4+}$ due to partial reduction in N_2 flow. The space group of $Ba_4YMn_3O_{11.5}$ is $R\bar{3}m$ referred as 12R whereas space group of $Ba_4YMn_3O_{11.5-\delta}$ is $P6_3/mmc$ referred as 6H. The very high dielectric constant of $Ba_4YMn_3O_{11.5-\delta}$ can be described by internal barrier layer capacitance (IBLC) effect in which semiconducting grains and insulating grain boundaries resulting charge storage capacity of grain increases due to grain boundaries. Due to variable oxidation state of Manganese oxygen vacancy created, which was induces phase transformation from 12-R to 6H and enhance its electrical, magnetic properties. The corner sharing of MnO_6 have Mn-O-Mn bond angle of 180° which facilitates super exchange interaction through oxide linkage (Mn^{3+}-O^{2-}-Mn^{3+}) all d^4 electrons of both manganese atom super-exchanged resulting antiferromagnetic character due to antiparallel alignment.

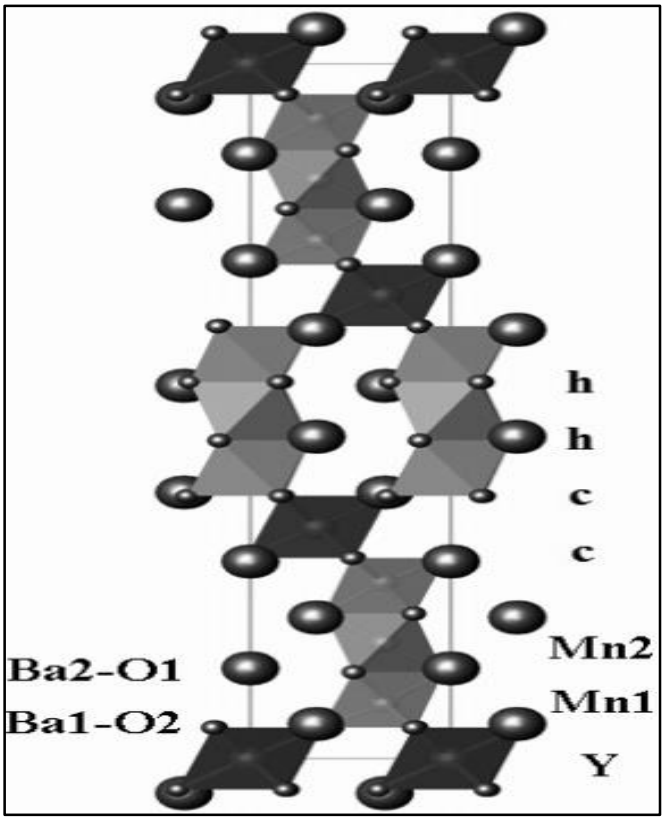

Figure 1.4 Crystal structure of $Ba_4YMn_3O_{11.5}$, Mn_3O_{12} trimers and YO_6 octahedra presented by gray and black respectively. The larger and small sphere represents Ba and O atoms respectively [Kuang *et al.* (2006)]

On the other hand, Mn^{3+}-O^{2-}-Mn^{4+} super-exchange results d^3 electron of Mn^{4+} super exchange with three electrons of d^4 of Mn^{3+} so one excess electron is responsible for ferromagnetic character.

1.10. Hexagonal Perovskite

For cubic perovskite structures tolerance factors is unity with A-O and B-O bond lengths follows Goldsmidts formula. If observed value of tolerance factor is either less or more than 1 indicates the structural deviation from ideal cubic system. If B-O bond length is higher than A-O then t< 1 which represents twisting of the BO_6 octahedra and monitor B-O-B bond angle are no longer equal to 180°. The strontium titanate $SrTiO_3$ adopts ideal cubic structure having t=1 in which bond angles Ti-O-Ti are 180° [Megaw (1946)] structure is represented in Figure 1.5. The ionic size of calcium is smaller than strontium so tolerance factor for $CaTiO_3$, t = 0.791 accommodated by twisting of TiO_6 octahedra shown in Figure 1.6, resulting Ti-O-Ti bond angles which are not equal to 180°. The ionic size of Ca^{2+} is less than Sr^{2+} [Koopmans *et al.* (1983)]. If A-O bond lengths increase relative to B-O bond length, tolerance factor greater than 1 is achieved. This indicates that the A cations are too large for the available sites in the cubic perovskite. No twisting can accommodate this, but in order to increase the average A site hexagonal close packing can be introduced into the stacking sequence of the AO_3 layers. Hexagonal close packing stacks the AO_3 layers in an ABAB sequence. The larger the value of *t*, the greater the proportion of AO_3 layers which are stacked using hexagonal close packing. This is exemplified by the $AMnO_3$ phases where A = Ca, Sr or Ba. As the size of the A cation increases, so does the tolerance factor increases therefore the proportion of AO_3 layers which are stacked using hexagonal close packing presented in Figure 1.7. $CaMnO_3$ has a tolerance factor of 0.987 and adopts a distorted cubic perovskite structure with only cubic close packing of the CaO_3 layers (and slight twisting of the MnO_6 octahedra) [Poeppelmeier *et al.* (1982)]. The barium cation is much larger than the calcium cation and this is reflected in the tolerance factor of $BaMnO_3$ (1.089). A hexagonal perovskite structure is adopted, in which the BaO_3

layers are all hexagonally close packed [Cussen and Battle (2000)]. In hexagonal perovskite structures the AO_3 layers are stacked along the *c* axis rather than the [111] stacking direction in the cubic system. The strontium cation is intermediate in size and the hexagonal perovskite structure adopted by $SrMnO_3$ contains 50% hexagonal close packing and 50% cubic close packing [Battle *et al.* (1988)].

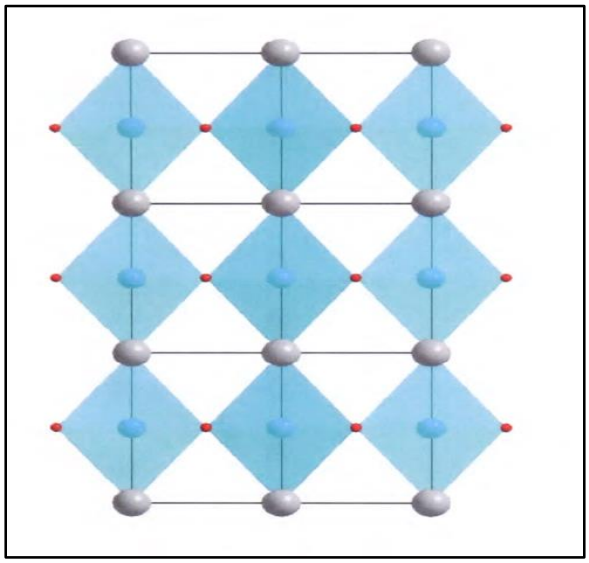

Figure 1.5 Ideal cubic structure of $SrTiO_3$ t=1.00

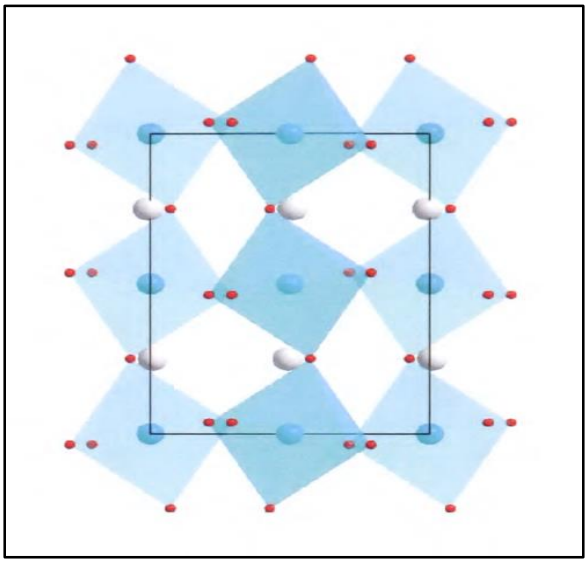

Figure 1.6 Distorted cubic structure of $CaTiO_3$ t= 0.791

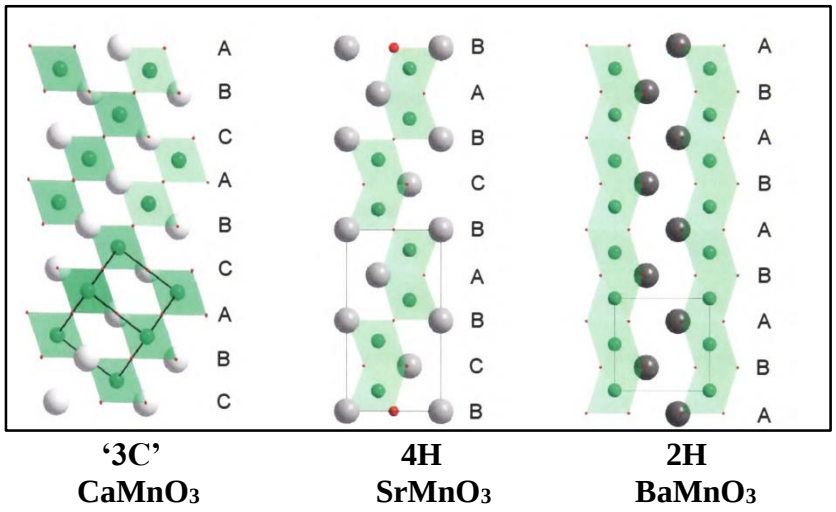

'3C' **CaMnO3**

4H **SrMnO3**

2H **BaMnO3**

Figure 1.7 Structures adopted by $AMnO_3$ (A= Ca, Sr or Br)

The first structural description of hexagonal was given by Katz and Ward according to this total number of close packed AO_3 layers stacked along with c axis in unit cell. Otherwise two

layers containing structure in unit cell referred as two-layer structure whereas manganese ions containing four-layer structure are labeled as 2H and 4H. According to Chamber land symmetry depends mainly on the symbol of the crystal system, the symbol H was used for structure having hexagonal space group such as two and four-layered structure whereas symbol R was used for rhombohedral space group.

1.10.1. Simple hexagonal perovskite structure

The hexagonal polymorphs have cubic layers into the hexagonal 2H stacking sequence. The apex sharing BO_6 octahedra link chains together. The stacking sequence minimizes the strain in structure. Some simple stacking sequences are listed in Table 1.3. The magnetic and dielectric properties of hexagonal perovskites mainly depend on nature of B cation. For example, 4H-$BaCrO_3$ is ferromagnetic and semiconducting, 4H-$SrMnO_3$ is antiferromagnetic insulator and 4H-$BaRuO_3$ is metallic.

Table 1.3 Simple stacking sequences of known hexagonal perovskites

Stacking sequence		**Name**	**c/(c+h)**	**Example**	**References**
5	chhhh	15R	0.200	$BaMnO_{3-x}$	[Negas and Roth (1971)]
4	chhh	6H	0.250	$BaMnO_{3-x}$	[Negas and Roth (1971)]
3	chh	9R	0.333	$BaMn_{1-x}Ir_xO_3$ (x=0.3,0.4 and 0.5)	[Jordan and Battle (2003)]
2,3	chchh	10H	0.400	$BaFeO_{2.67}$ $BaIr_{1-x}CoO_{3-\delta}$ $Ba_5Co_5ClO_{13}$	[De Muro *et al.* (2005)], [Vente and Battle (2000)] [Yamaura *et al.* (2001)]
2	ch	4H	0.500	$BaRuO_3$	**[**Rijssenbeek *et al* (1998)]
1,2,2,2,2	cchchchch	27R	0.556	$BaCrO_3$	[Haradem *et al* (1980)]
1,2,2,2	cchchch	14H	0.571	$BaCrO_3$	[Haradem *et al* (1980)]
1,2,2	cchch	15R	0.600	$BaFe_{0.7}Ir_{0.3}O_{2.949}$	[Jordan *et al* (2003)]
1,2	cch	6H	0.666	$Ba_3MRu_2O_9$ (M= Fe, Co, Ni, Cu and In)	[Rijssenbeck *et al* (1998)]
1,1,2,1,2	ccchcch	21R	0.714	$BaRu_{0.57}Li_{0.428}O_{2.857}$	[Stitzer *et al* (2003)]
1,1,2	ccch	8H’	0.750	$BaCr_{0.5}(Nb/Ta)_{0.5}O_3$	[Choy *et al* (1996)]
1,1,1,2	cccch	10H	0.800	$SrMn_{0.72}Fe_{0.27}O_{2.87}$	[Battle *et al* (1996)]
1,1,1,1,2	ccccch	12H’	0.833	$BaTi_{0.67}(Y,Nd)_{0.33}O_{2.83}$ $Ba(Mn,V,As,P,Cr)_{0.33}(Ru/Nb/Ta)_{0.33}Na_{0.33}O_{2.83}$	[Kuang *et al* (2002)] [Quarez *et al* (2003)]

1.11. Ferroelectricity

It is a property of material which has spontaneous electric polarization that can modulate by application of external electric field. Ferroelectricity was discovered in 1920 in Rochelle salt by Valasek. Ferroelectric materials have permanent internal dipole moment which can be align in presence of electric field. The unusual dielectric constant of Barium titanate is due to its ferroelectric behavior. In ferroelectric material atoms are displaced in a particular orientation from their original lattice point resulting spontaneous polarization due to non-centrosymmetric structure.

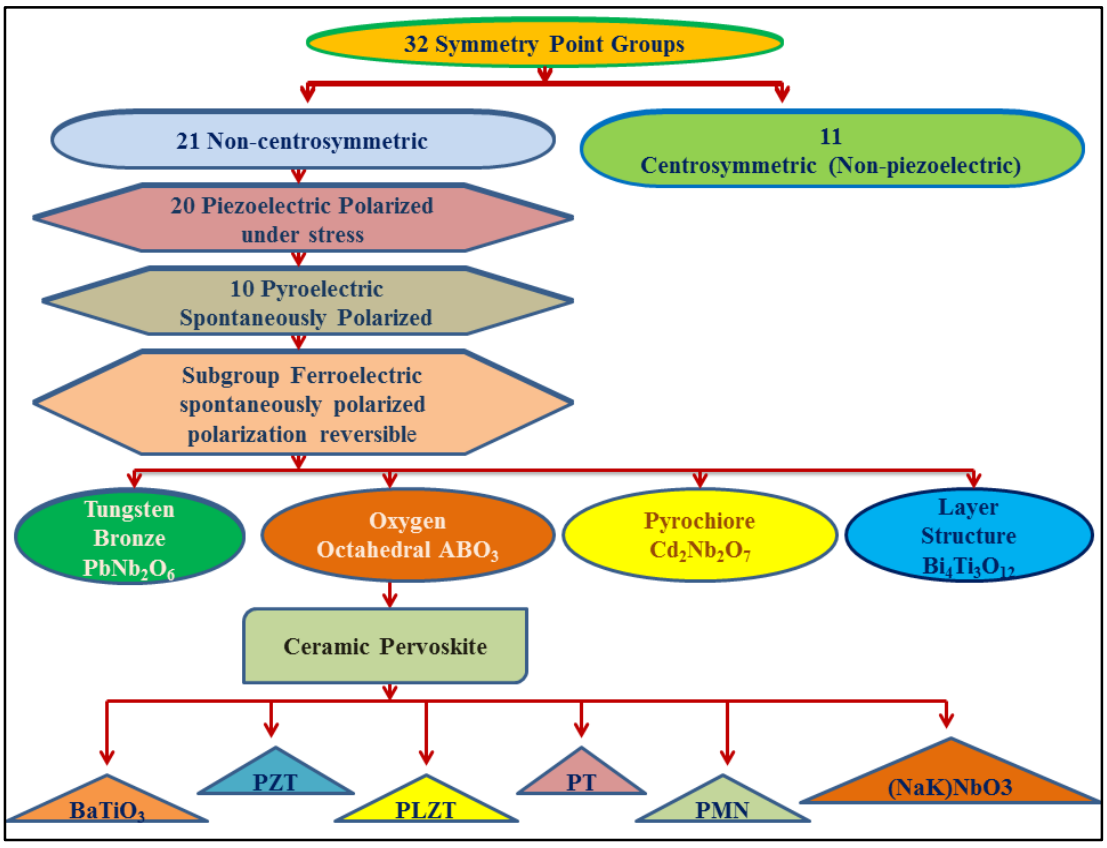

Figure 1.8 Flow chart diagram of ferroelectric subgroups

In Figure 1.8 all 32-point group are subdivided in to seven crystal systems as triclinic, monoclinic, orthorhombic, tetragonal, rhombohedral, hexagonal and cubic. Of the 32 point groups, noncentrosymetric classes are 21 in which 20 are piezoelectric and one is not piezoelectric due to absence of center of symmetry. Out of 20, ten crystal classes are pyroelectric, means these materials permanently polarized in certain temperature range. Piezoelectric class generates polarization by stress while in pyroelectric create permanent dipoles which changes with temperature. The spontaneously polarized pyroelectric materials are further categorized in sub group known as ferroelectric materials. Ferroelectric materials have spontaneous polarization as well as reorientation of polarization on application of electric field. Four types of ferroelectric ceramics are sub categorized like tungsten-bronze group, oxygen octahedral, pyrochlore and bismuth layer structure group. The perovskite ABO_3 is very important category in which barium titanate, PZT, PLZT and PMN shows very interesting ferroelectric properties. In PLZT Pb^{2+} and La^{3+} present at A site whereas Zr^{4+} and Ti^{4+} situated at B site of ABO_3 perovskite oxides when external electric field is applied the position of Zr^{4+} and Ti^{4+} shift towards field resulting polarization. The shifting of metal ions occurs along c axis in tetragonal structure, whereas in orthogonal, displacement along a or b axis is also observed. The polarization up and polarization down represents 180° polarization reversal. The particular area of material having same orientation of polarization referred as domain, domain walls separate the domains having different orientation of polarization. The conclusion drawn from the figure is that all ferroelectrics are piezoelectric but all piezoelectric are not ferroelectric.

1.11.1. Hysteresis loop: the fingerprint of ferroelectricity

The term ferroelectric was obtained from similar magnetic loop (M-H) in ferromagnetic material with exception of iron is not present in ferroelectric materials. From the symmetric P-E (polarization versus electric field) hysteresis loop, the remanent polarization and coercive field were determined. Polarization at zero field is known as remanent polarization whereas coercive field is the value of field at zero polarization [Ghosh *et al.* (2016)]. The P-E hysteresis loop must show saturation polarization and concave region in P versus E plot as shown in Figure 1.9.

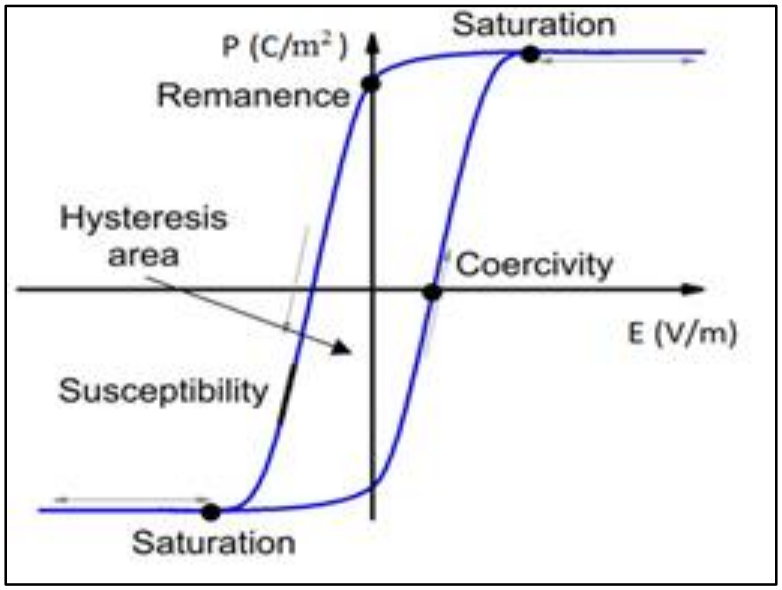

Figure 1.9 PE hysteresis loop

1.11.2. Ferroelectric domain

Similar polarization orientation present in volume region of material is known as ferroelectric domains. The energy of domains is same at zero filed and strain free condition whereas on application of electric field all domains are align in the direction of field. At very high field permanent reorientation of polarization of domains observed. Ferroelectric materials are very important category of materials which shows wide range of applications like actuators, ultrasonic transducers, paraelectric detectors, piezoelectric sonar, high dielectric capacitors and ferroelectric memories [Haertling (1999), De *et al.* (2015)].

1.12. Magnetic properties

Magnetic properties of ceramic are very important class of materials which have variety of application such as data storage, tunnel junction and spin valves. The magnetic ceramic materials have some special properties like magnetic coupling, low loss and high electrical resistivity which were altered by structure and composition of materials [Ahmed *et al.* (2004)]. As the particle size is less than 100 nm large number of atoms are found on the surface of the nanocrystals, so magnetic structure changes in nanoscale region as compared to bulk material. The magnetic properties of nanoparticles are affected by particle size, morphology, synthesis route and chemical composition.

1.12.1. Origin of magnetism

The materials having unpaired electrons in orbitals spin either clockwise or anticlockwise and orbitals also spin around the nucleus results magnetic moments [Jiles (2015),

McCurrie (1994)]. If electrons are paired means they spin in opposite direction their resulting moments cancels each other whereas unpaired electrons have a magnetic moment.

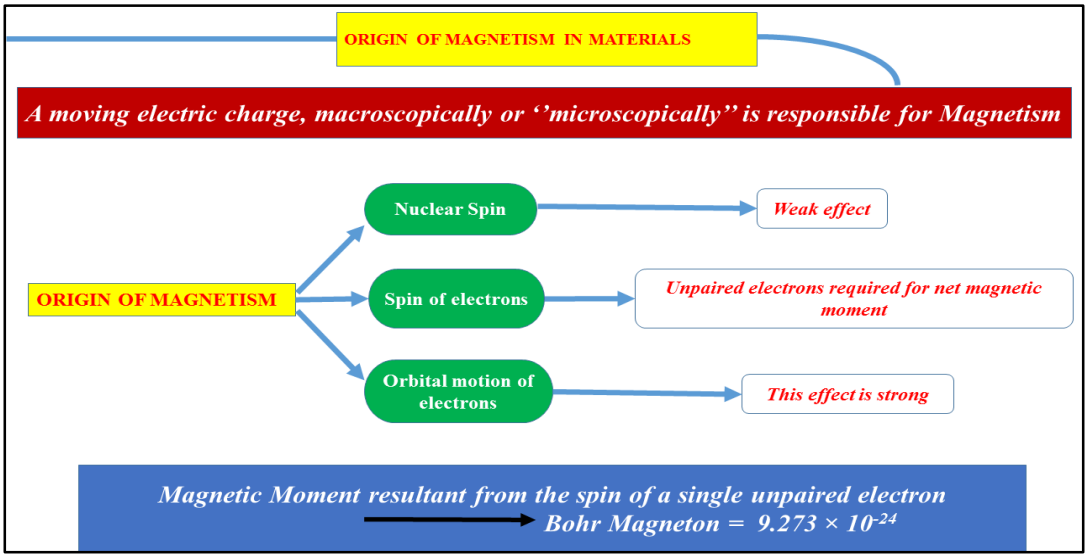

Figure 1.10 Flow chart of origin of magnetism in materials

The induced magnetic field (B) of material on application of external magnetic field (H) can be expressed by equation (1.10)

$$B = H+4\pi M \qquad (1.10)$$

Where M is intensity of magnetization express in terms of magnetic moment per unit volume and is given by equation (1.11)

$$M = m/V \qquad (1.11)$$

Where, V is the volume of the substance. The specific magnetization (σ) is given by equation (1.12)

$$\sigma = m/W = M/\rho \ (emu/g) \qquad (1.12)$$

Where, W is the mass and ρ is the density of the material.

The investigation of magnetic properties of material is not only intensity of magnetization but gradually applying of magnetic field change intensity of magnetization (M versus H) and also magnetization with temperature (M versus T) at constant field.

The magnetization per unit magnetic field is called the magnetic susceptibility (κ) (equation (1.13))

$$\kappa = M/H \ (emu/cm^3Oe) \qquad (1.13)$$

The ratio of magnetic induction to an applied magnetic field is a material's permeability (P) and given by (equation (1.14))

$$P = 1+4\pi\chi_{mol} \qquad (1.14)$$

where χ_{mol} is a material's molar susceptibility and described as (equation (1.15))

$$\chi_{mol} = \kappa F/\rho \qquad (1.15)$$

F is the formula weight of the material and ρ is its density. Depending on the values and orders of susceptibility, substances are classified into certain categories.

1.12.2. Types of magnetic materials

Depending on the alignment of magnetic moments with or without external magnetic field, magnetism is classified in three parts.

(i) Diamagnetism

It is a week form of magnetism which arises due to change in the orbital motion of electrons on application of magnetic field. There are no magnetic dipoles in absence of field, when external magnetic field applied then all magnetic dipoles align in opposite to field direction as shown in Figure 1.11. The materials having paired electrons shows opposite spins

cancel out resulting magnetic dipole. Diamagnetic materials feel repulsion in external magnetic field. Diamagnet is expelled in strong applied magnetic field and magnetic susceptibility is less than one [Schenck (2005)].

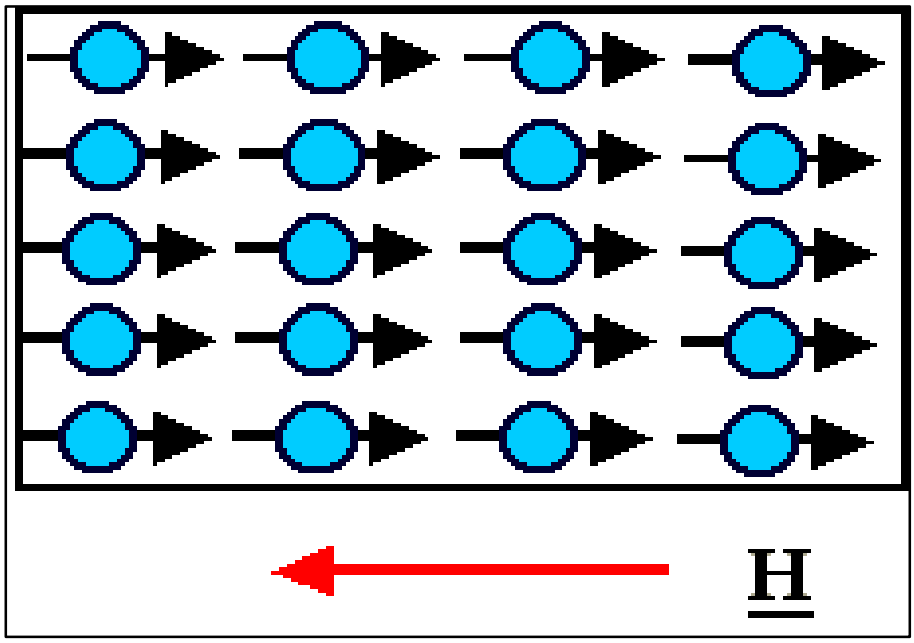

Figure 1.11 Diamagnetic material

(ii) Paramagnetism

The materials having unpaired electrons show paramagnetism due to incomplete cancelation of magnetic dipoles. The random alignment of magnetic moment causes no net magnetization in absence of magnetic field. On application of external field, orientation of magnetic moment towards field direction results very large magnetic moment as shown in Figure 1.12. These materials attract in external applied magnetic field. If temperature of

material increases, then randomness of magnetic moments increases thus susceptibility decreases [Cullity (2011)].

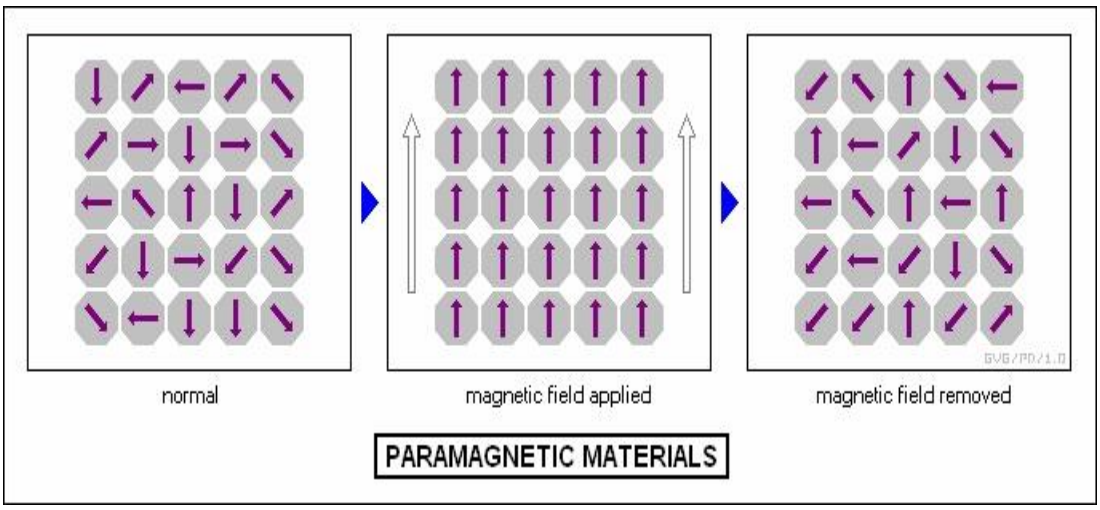

Figure 1.12 Paramagnetic material

Curie law describes effect of temperature on susceptibility having relation shown in equation (1.16).

$$\chi = C/T \qquad (1.16)$$

Where χ is susceptibility of material, C is the Curie constant and T temperature. The equation indicates inverse relation between paramagnetic susceptibility and temperature thus materials are more magnetized at low temperature. Curie law is applicable for that system which contains non-interacting magnetic moments. Magnetic susceptibility of paramagnetic materials is greater than one. Weis law is the modified Curie law by using molecular field (equation (1.17)).

$$\chi = C/T - \theta \qquad (1.17)$$

where θ is measure of the magnetic interaction strength.

(iii) Ferromagnetism

The materials having permanent magnetic moment in absence of external magnetic field comes under ferromagnetism. Permanent magnetic moment arises due to uncancelled electron spins. The alignment of moment creates by coupling interaction of electron spins of adjacent atoms with other. Regular arrangement of magnetic moment suggests spontaneous magnetic moment. As temperature increases these magnetic arrangements disordered due to thermal agitation resulting ferromagnetic property changes in to paramagnetic. The temperature at which ferromagnetic changes to paramagnetic known as Curie temperature (Tc), bellow Tc materials behaves as ferromagnetic whereas above Tc material behave like paramagnetic [Bakonyi *et al.* (2005)]. Ferromagnetic materials exhibit magnetic moments alignment in small region is known as domains. The domains are separated by domain boundary and change in direction of magnetization across boundary as shown in Figure 1.13. The vector sum of domains gives magnitude of magnetization.

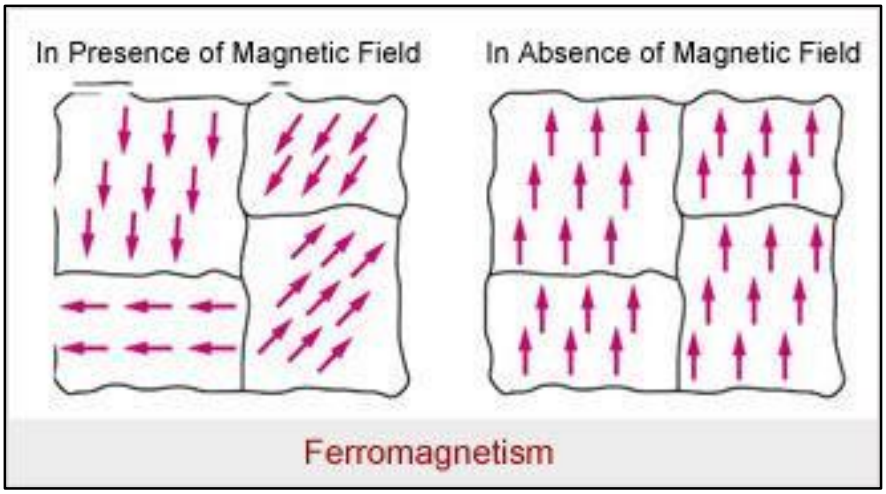

Figure 1.13 Ferromagnetic material

(iv) Antiferromagnetism

The materials have magnetic interaction between any two dipoles align themselves anti-parallel to each other so all dipoles have equal magnitude resulting zero magnetization as shown in Figure 1.14. The magnetic susceptibility of antiferromagnetic materials is very small and positive. Below Neel temperature (T_N) net magnetic moment is zero whereas above Neel temperature antiferromagnetic material becomes paramagnetic due to thermal agitation, which destroys alignment of magnetic moments. [Matsumoto *et al*. (2002)].

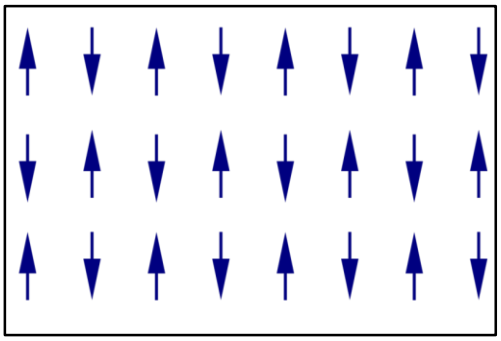

Figure 1.14 Antiferromagnetic material

(v) Ferrimagnetism

The materials have their magnetic moments aligned in such a way that the moments do not completely cancel out and resulting net magnetization remains at even no external field is applied as shown in Figure 1.15. Magnitude of magnetic moments is different but aligns in opposite direction. Ferrite and garnet are example of ferromagnetic materials which behaves paramagnetic above Curie temperature [Özgür *et al.* (2009)].

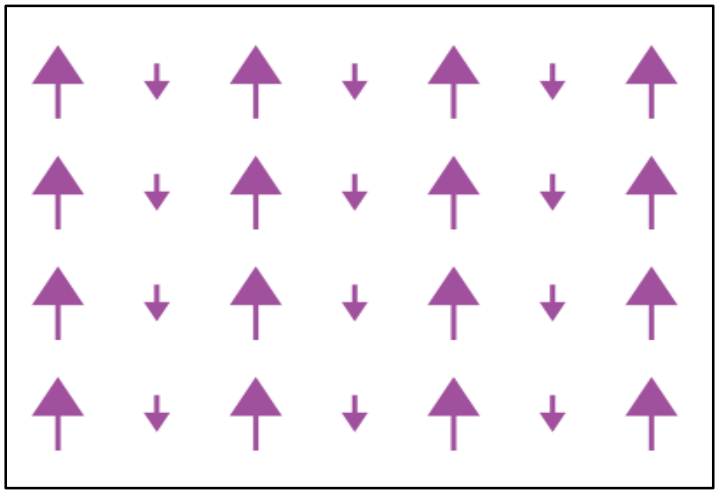

Figure 1.15 Antiferrimagnetic material

1.12.3. Superparamagnetism

Superparamagnetism appears in very fine magnetic nanoparticle as small ferromagnetic or ferromagnetic [Liu *et al* (2000), Song and Zhang (2004)]**.** Magnetization randomly flips direction under influence of temperature and time taken by two flips is known as Neel relaxation time. Superparamagnetic materials have zero remanent and coercivity. Superparamagnetic materials are widely used in magnetic resonance imaging, drug delivery, magnetic hyperthermia **[**Batlle *et al.* (1988)]. Superparamagnetism present in nanoparticle (3-50 nm) behaving single magnetic domain [Goya *et al*. (2003)]. The magnetic moment of nanoparticles usually has two stable antiparallel orientations which were separated by energy barrier. If energy barrier is greater than thermal energy, then magnetization is blocked spontaneous reversal becomes negligible [Bowles *et al*. (2010)]. On the other hand, barrier are relatively low, thermal excitation creates magnetization reversal in short time and grains comes under superparamagnetic state. The temperature at which maximum magnetic moment observed is known as blocking temperature (T_B). Below blocking temperature material behaves like ferromagnetic whereas above blocking temperature superparamagnetic [Koseoglu

et al. (2011)]. Blocking temperature highly depends on particle size of material and decreases with increase in size of particles [Kodama *et al.* (1997)]. The relation between blocking temperature with particle volume is shown in equation (1.18). Figure 1.16 shows the characteristic M-H hysteresis loop of ferromagnetism, paramagnetism and superparamagnetism.

$$T_B = KV/25k_B \qquad (1.18)$$

Where K is an anisotropy constant, V is the volume of the particle and k_B is the Boltzmann constant (1.38×10^{-23} J K^{-1}).

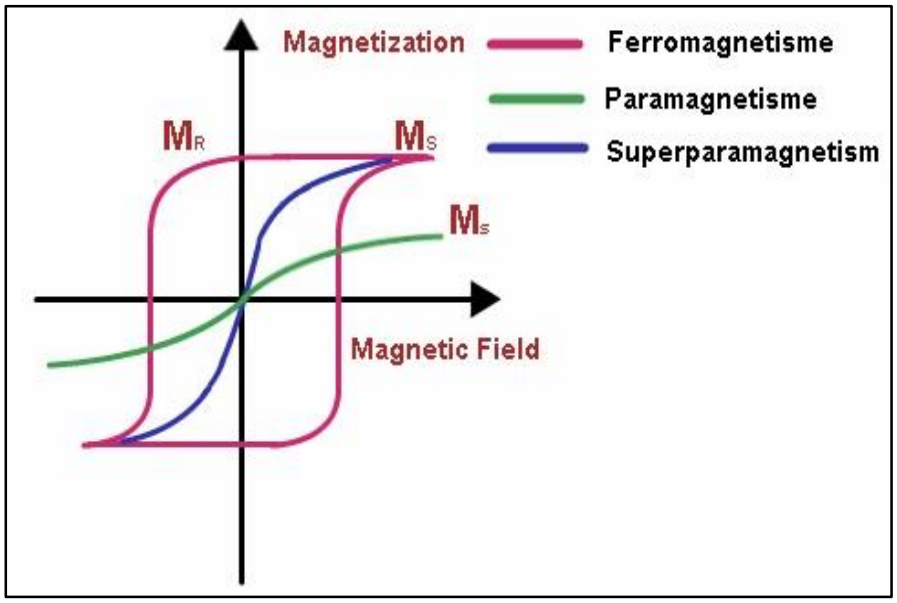

Figure 1.16 M-H hysteresis

1.12.4. Magnetic Superexchange

In perovskite oxides magnetic metal ions are joined with oxide ions therefore direct exchange are not possible. Many indirect coupling of magnetic moments are possible through oxide linkage that is cation-oxygen-cation superexchange as shown in Figure 1.17. The bond angle of cation-oxygen-cation is supposed to be 180°. In exited state one p electron of oxygen ions (O^{2-}) transfer to d orbital of neighbouring metal ion resulting paramagnetic behavior of oxygen which take part in magnetic interaction [Anderson (1950)]. The ferromagnetic or antiferromagnetic alignment occurs by superexchange.

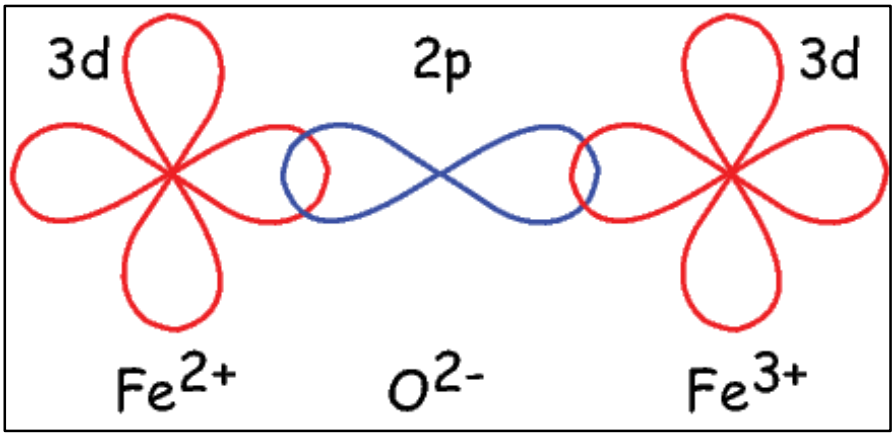

Figure 1.17 Supper exchange interaction

The electron transfers between eg energy state of d orbital and pσ orbitals are known as σ transfer whereas between eg and pπ orbitals called π transfer. Covalency of sigma bond contributes more towards super-exchange, as ionic character increases superexchange decreases. The electronic superexchange control by correlation effect in which simultaneous bond formation on each side of oxide ion and delocalization effect consider the transfer of electron from one cation to other through anion [Suaud *et al.* (2002)]. The extent of orbital

overlap controls the delocalization. If both cations have half field eg orbitals so anions electrons of antiparallel spin couple on both side which creates strong antiferromagnetic interaction between cations. If one cation has half field eg orbital and other is empty, then anion electron couple anti parallel spin with half field cation whereas parallel spin couple with empty cation resulting ferromagnetic interactions. The effect of temperature and field dependent magnetization of ferroelectric is necessary to understand. Bellow Curie temperature and absence of field magnetization develops due to coupling such type of magnetization is known as spontaneous magnetization (Ms) [Sarma *et al.* (2003)]. For ferromagnetic materials spontaneous magnetization is equal to saturation magnetization at T=0 K.

1.13. Aim of study

Nowadays, use of electronic devices (mobiles, camera, computers, Television etc) is very demanding requires continuous improvement in miniaturization of these devices. The memory and energy storage devices demanding high dielectric constant and low loss material, scientist taking interest regarding to serve better microelectronic devices.

(i) The work of thesis focuses synthesis and characterization of ceramic materials. Studied various application like dielectric, ferroelectric, and magnetic properties of material and its dependence on temperature and frequency. Effect of doping at titanium and manganese site by iron on synthesis and dielectric, ferroelectric and magnetic properties were reported.

(ii) Separate contribution of grain and grain boundary, microstructure, particle shape, temperature and frequency on dielectric, ferroelectric and magnetic properties are studied in details.

(iii) To get good quality of ceramic materials chemical method and semi wet route are used to monitor homogeneous mixing of metal ions and material synthesized at low sintering temperature as well as less duration. In order to get high dielectric constant and low dielectric loss the synthesized materials $Ba_4YMn_3O_{11.5-\delta}$ (BYMO) and $Ba_6Y_2Ti_4O_{17}$ (BYTO) are used as capacitor and memory storage devices.

The objective of present work is to synthesize following ceramic materials and effect of doping of Fe in BYMO and BYTO by below mentioned synthesis route.

- $Ba_4YMn_3O_{11.5-\delta}$ (BYMO) by chemical route
- $Ba_4YMn_{2.95}Fe_{0.05}O_{11.5}$ (BYMFO-05) by chemical route
- $Ba_4YMn_{2.90}Fe_{0.1}O_{11.5}$ (BYMFO-1) by chemical route
- $Ba_4YMn_{2.80}Fe_{0.2}O_{11.5}$ (BYMFO-2) by chemical route
- $Ba_6Y_2Ti_4O_{15}$ (BYTO) by semi wet route
- $Ba_6Y_2Ti_{3.95}Fe_{0.05}O_{15}$ (BYTFO-05) by semi wet route
- $Ba_6Y_2Ti_{3.90}Fe_{0.1}O_{15}$ (BYTFO-1) by semi wet route
- $Ba_6Y_2Ti_{3.80}Fe_{0.2}O_{15}$ (BYTFO-2) by semi wet route

These ceramics were characterized by different physiochemical techniques like TG/DTA, XRD, SEM-EDX and TEM. The dielectric ferroelectric and magnetic properties will be studied as a function of temperature and frequency.